Interfaces of polydisperse fluids : surface tension and adsorption properties

L. Bellier-Castella[1], H. Xu [1] and M. Baus [2]

(February 1, 2008)

[1] Département de Physique des Matériaux (UMR 5586 du CNRS),
Université Claude Bernard-Lyon1, 69622 Villeurbanne Cedex, France
[2] Physique des Polymères, Université Libre de Bruxelles,
Campus Plaine, CP 223, B-1050 Brussels, Belgium

PACS numbers: 64.75.+g, 68.05.-n, 64.10.+h

We consider a system of spherical colloidal particles with a size polydispersity and use a simple van der Waals description in order to study the combined effect of both the polydispersity and the spatial non-uniformity induced by a planar interface between a low-density fluid phase (enriched in small particles) and a high-density fluid phase (enriched in large particles). We find a strong adsorption of small particles at the interface, the latter being broadened with respect to the monodisperse case. We also find that the surface tension of the polydisperse system results from a competition between the tendancy of the polydispersity to lower the surface tension and its tendancy to raise the critical-point temperature (i.e. its tendancy to favor phase separation) with the former tendancy winning at low temperatures and the latter at the higher temperatures.

I. INTRODUCTION

Many of the complex fluids used in the industry or in the soft condensed matter physics laboratory are collections of nearly identical particles which exhibit one or several polydispersities, i.e. properties such as the size or the shape of these particles which are distributed whithin some interval in an almost continuous manner [1]. These fluids are hence continuous mixtures of similar particles and it is of some practical importance to know how their composition or polydispersity influences their physical properties, e.g. their phase behavior and rheological properties. Here we will be concerned only with the equilibrium phase behavior of such polydisperse fluids. The generalization of the well-established methods for the study of phase transitions in discrete mixtures to continuous mixtures is a technically very demanding task which has recently become an active area of research [2]. Most of this research has been limited to spatially uniform (or bulk) phases while it is our purpose here to extend it further to non-uniform situations involving the interface between two coexisting bulk phases. Such an intrinsic interface is different from, e.g. the interface between a bulk phase and a substrate (see [3] for some preliminary work in this direction). Indeed, in the latter case the interface can be characterized thermodynamically by a surface excess free- energy defined relative to the substrate whereas in the former case it is characterized by a surface tension (which is both a surface free-energy and a thermodynamic force) defined with respect to an intrinsic "surface of tension" [4]. We will hence be particularly interested in the influence of the polydispersity on this interfacial surface tension.

In order to keep the problem manageable we will restrict ourselves to the fluid phases of a system of spherical particles with a size-distribution, a situation typical for many colloidal dispersions [5]. The initial or parent-phase size-distribution will be assumed to be fixed once and for all by the production process of the colloidal particles and taken to be of the monomodal type, i.e. peaked around a single reference species, such as is appropriate for the polydisperse generalization of a one-component system. When this (initial) parent-phase is put into appropriate thermodynamic conditions it will phase separate or " fractionate" into two (or more [6]) daughter-phases. Since these daughter-phases differ in density and composition an interface will build up between them across which the properties of one bulk phase transform continuously into those of the coexisting bulk phase. The properties of such a spatially non-uniform two-phase system are most conveniently studied in two steps. First, one determines the two spatially uniform bulk phases which are able to coexist in equilibrium. Next, one determines the profiles across the interface of those properties which are spatially varying in the two-phase system. For the first step we will use the results of our earlier study [7] based on the van der Waals (vdW) free-energy of a polydisperse system of spherical colloidal particles interacting via excluded volume repulsions and

vdW-like attractions. Such a description is of course not exact but simplifies considerably the technical problems raised by the study of phase equilibria in polydisperse systems. For the second step we will use an earlier extension of the vdW free-energy to spatially non-uniform systems [8] and generalize it here to polydisperse systems. In order to extract the surface tension we will, finally, adapt to the present case a general procedure advocated elsewhere [9].

In Sec. II we introduce the vdW density functional of a spatially non-uniform polydisperse system. The density profiles across a planar interface are computed in Sec. III while the corresponding adsorption properties will be discussed in Sec. IV. The pressure profiles across the planar interface are determined in Sec. V while the resulting surface tension is presented in Sec. VI. Our conclusions follow in the final Sec. VII.

II. THE SPATIALLY NON-UNIFORM POLYDISPERSE SYSTEM

The equilibrium properties of spatially non-uniform systems (e.g. interfaces) are most easily studied within density functional theory (DFT) [10]. The starting point of DFT is the variational free-energy, $A(T,[\rho],[\Phi])$:

$$A(T,[\rho],[\Phi]) = F(T,[\rho]) + \int d\mathbf{r} \int d\sigma\, \rho(\mathbf{r},\sigma)\{\Phi(\mathbf{r},\sigma) - \mu(\sigma)\} \quad (1)$$

where T is the equilibrium temperature, $F(T,[\rho])$ the intrinsic Helmholtz free-energy viewed as a functional (indicated as $[\rho]$) of the average local number density, $\rho(\mathbf{r},\sigma)$, $\mathbf{r}$ being the position variable (assuming spherical particles) and σ the (dimensionless) polydispersity variable, $\mu(\sigma)$ is the chemical potential of species σ and $\Phi(\mathbf{r},\sigma)$ the one-body external field responsible for the spatial non-uniformity of the system (the functional dependence of A on $\Phi(\mathbf{r},\sigma)$ being indicated as $[\Phi]$). The equilibrium density, $\rho(\mathbf{r},\sigma)$, corresponding to a given $\Phi(\mathbf{r},\sigma)$, can then be obtained by solving the Euler-Lagrange equation :

$$\frac{\delta A(T,[\rho],[\Phi])}{\delta\rho(\mathbf{r},\sigma)}|_{T,[\Phi]} = 0 \quad (2)$$

corresponding to (1), viz. :

$$\mu(\sigma) = \Phi(\mathbf{r},\sigma) + \frac{\delta F(T[\rho])}{\delta\rho(\mathbf{r},\sigma)}|_T\,. \quad (3)$$

Eq. (3) expresses the fact that in equilibrium the chemical potential $\mu(\sigma)$ of each species σ has to remain constant in space. In the present study, $F(T,[\rho])$, will be approximated by the following vdW-type expression [7,8,11] :

$$\begin{aligned} F(T,[\rho]) = k_B\,T \int d\mathbf{r} \int d\sigma \rho(\mathbf{r},\sigma) \\ \{\ln(\frac{\Lambda^3(\sigma)\rho(\mathbf{r},\sigma)}{E(\mathbf{r},[\rho])}) - 1\} \\ +\frac{1}{2}\int d\mathbf{r}\int d\sigma \int d\mathbf{r}' \int d\sigma'\, \rho(\mathbf{r},\sigma) \\ V_A(|\mathbf{r}-\mathbf{r}'|;\sigma,\sigma')\rho(\mathbf{r}',\sigma') \end{aligned} \quad (4)$$

where k_B is Boltzmann's constant, $\Lambda(\sigma)$ the thermal de Broglie wavelength of species σ, $V_A(r;\sigma,\sigma')$ the potential of attraction between two particles of species σ and σ' a distance $r = |\mathbf{r}|$ apart, while $E(\mathbf{r},[\rho])$ represents the excluded volume correction resulting from the repulsions :

$$E(\mathbf{r},[\rho]) = 1 - \int d\sigma v(\sigma)\rho(\mathbf{r},\sigma), \quad (5)$$

$v(\sigma) = \frac{4\pi}{3}R^3(\sigma)$ being the volume of a spherical particle of radius $R(\sigma)$. It should be noted that, as is usual in this context [11], σ is used here both as a species label and as the (dimensionless) polydispersity variable, $R(\sigma)/R(1)$, $R(1)$ being the radius of the reference species $\sigma = 1$. From (4) we obtain for (3) :

$$\begin{aligned} \mu(\sigma) = \Phi(\mathbf{r},\sigma) + k_B\,T\ln(\frac{\Lambda^3(\sigma)\rho(\mathbf{r},\sigma)}{E(\mathbf{r},[\rho])}) \\ +k_B\,T\frac{v(\sigma)}{E(\mathbf{r},[\rho])}\int d\sigma'\rho(\mathbf{r},\sigma') \\ +\int d\mathbf{r}'\int d\sigma'\, V_A(|\mathbf{r}-\mathbf{r}'|;\sigma,\sigma')\rho(\mathbf{r}',\sigma'). \end{aligned} \quad (6)$$

The above represents a straightforward extension of DFT to continuous mixtures while (4-5) reduces to the vdW free-energy used in [7] for the uniform polydisperse system as well as to the vdW free-energy used in [8] for the non-uniform monodisperse system. Both approximations reducing to the usual vdW free-energy for the uniform monodisperse system. The basic physics of the vdW approximation being, as usual, the correction of the ideal gaz behavior for the finite size of the particles via the excluded volume correction (E) and the inclusion of the cohesion between the particles via the interparticle attractions (V_A), as described here respectively by the first and second term of (4). Of course, more involved expressions of $F(T,[\rho])$ are available but these can only add further complications to the already fairly complex calculations required by the present combination of the non-uniformity with the polydispersity of the system. Past experience has shown however that the present vdW approximation is able to capture the essence of the underlying phase behavior in a qualitatively correct manner [12]. In [7] we have studied several model-polydispersities differing in the σ-dependence of $v(\sigma)$ and $V_A(r;\sigma,\sigma')$. It

was found there that the model based on the simple approximation :

$$v(\sigma) = v(1), \;\; V_A(r;\sigma,\sigma') = \sigma\,\sigma'\,V_A(r;1,1) \tag{7}$$

has a phase behavior which is similar to that of the more involved expressions but is simpler to study. Henceforth we will use thus (4-5) together with (7). The physical contents of (7) reflects the fact (cf. [7]) that the amplitude-polydispersity of $V_A(r;\sigma,\sigma')$ dominates the volume-polydispersity of $v(\sigma)$. The inclusion of the volume-polydispersity of $v(\sigma)$ will therefore not alter qualitatively our conclusions.

III. THE PLANAR INTERFACE

We will consider a planar interface perpendicular to the z-axis. Translational invariance in the (x,y)-directions implies then, $\rho(\mathbf{r},\sigma) \to \rho(z,\sigma)$ and $\Phi(\mathbf{r},\sigma) \to \Phi(z,\sigma)$, so that the Euler-Lagrange eq. (6) can be rewritten, after separating the local (in z) and non-local contributions, as :

$$\mu(\sigma) = \Phi(z,\sigma) + \mu_0(z,\sigma;T,[\eta]) + \sigma\int_{-\infty}^{\infty} dz'\,V_1(|z-z'|)\,\{\eta_1(z') - \eta_1(z)\} \tag{8}$$

with $\mu_0(z,\sigma;T,[\eta])$ a shorthand notation for :

$$\mu_0(z,\sigma;T,[\eta]) = k_B\,T\ln\frac{\Lambda^3(\sigma)}{v(1)} + k_B\,T\ln\frac{\eta(z,\sigma)}{1-\eta_0(z)} + k_B\,T\frac{\eta_0(z)}{1-\eta_0(z)} + \sigma\,V_0\,\eta_1(z) \tag{9}$$

where

$$\eta(z,\sigma) = v(1)\,\rho(z,\sigma), \;\; \eta_0(z) = \int d\sigma\,\eta(z,\sigma), \;\; \eta_1(z) = \int d\sigma\,\sigma\,\eta(z,\sigma), \tag{10}$$

are the dimensionless density and polydispersity moments, whereas :

$$v(1)\,V_1(|z|) = \int_{-\infty}^{\infty} dx \int_{-\infty}^{\infty} dy\,V_A(r;1,1), \;\; v(1)\,V_0 = \int d\mathbf{r}\,V_A(r;1,1), \tag{11}$$

with $\sigma = 1$ denoting the reference particle of volume $v(1)$. The external (symmetry breaking) field, $\Phi(z,\sigma)$, will as usual be replaced by boundary conditions. We thus consider eq. (8) without external field, viz. :

$$\mu(\sigma) = \mu_0(z,\sigma;T,[\eta]) + \sigma\int_{-\infty}^{\infty} dz'\,V_1(|z-z'|)\,\{\eta_1(z') - \eta_1(z)\} \tag{12}$$

and require that for, $z \to \pm\infty$, the solution $\eta(z,\sigma)$ of (12) matches the bulk-phase densities, say $\eta_\pm(\sigma)$, or $\eta(z=\pm\infty,\sigma) = \eta_\pm(\sigma)$. These bulk-phase densities must hence satisfy eq. (12) for $z = \pm\infty$. Taking the limit of (12) for $z \to \pm\infty$, the second term in its r.h.s. will vanish and we obtain :

$$\mu(\sigma) = \mu_0(z=\pm\infty,\sigma;T,[\eta_\pm]) \tag{13}$$

i.e., the chemical potential of species σ in the non-uniform system must be constant and equal to the chemical potential of species σ in the two bulk-phases. Indeed, evaluating the r.h.s. of (13) from (9) for $\eta(z=\pm\infty,\sigma) = \eta_\pm(\sigma)$ we obtain :

$$\mu_0(\pm\infty,\sigma;T,[\eta_\pm]) = k_B\,T\ln\frac{\Lambda^3(\sigma)}{v(1)} + k_B\,T\ln\frac{\eta_\pm(\sigma)}{1-\eta_0^\pm} + k_B\,T\frac{\eta_0^\pm}{1-\eta_0^\pm} + \sigma\,V_0\,\eta_1^\pm \tag{14}$$

where :

$$\eta_0^\pm = \int d\sigma\,\eta_\pm(\sigma), \;\; \eta_1^\pm = \int d\sigma\,\sigma\,\eta_\pm(\sigma) \tag{15}$$

while the r.h.s. of (14) represents (cf. [7]) the chemical potential of a uniform phase of density $\eta_\pm(\sigma)$. When the two bulk phases are in equilibrium, the chemical potential of the $\eta_+(\sigma)$ phase must be equal to that of the $\eta_-(\sigma)$ phase, hence (13) will be satisfied. Eq. (13) allows us to elimite $\mu(\sigma)$ from (12) and rewrite it as :

$$\mu_0(\pm\infty,\sigma;T,[\eta_\pm]) - \mu_0(z,\sigma;T,[\eta]) = \sigma\int_{-\infty}^{\infty} dz'\,V_1(|z-z'|)\,\{\eta_1(z') - \eta_1(z)\} \tag{16}$$

an integral equation for $\eta(z,\sigma)$ incorporating the boundary conditions. On using (9) and (14) we can rewrite (16) as :

$$\eta(z,\sigma) = A_0^\pm(z) M^\pm(z,\sigma) \tag{17}$$

where $A_0^\pm(z)$ is a shorthand notation for :

$$A_0^\pm(z) = \frac{1-\eta_0(z)}{1-\eta_0^\pm}\,\exp\{\frac{1}{1-\eta_0^\pm} - \frac{1}{1-\eta_0(z)}\} \tag{18}$$

and $M^\pm(z,\sigma)$ for :

$$M^\pm(z,\sigma) = \eta_\pm(\sigma)\exp\,\sigma\int_{-\infty}^{\infty} dz'\,\beta\,V_1(|z-z'|)\,\{\eta_1^\pm - \eta_1(z')\} \tag{19}$$

where $\beta = 1/k_BT$. Taking now the first two σ-moments of (17) yields a system of two integral equations for $\eta_0(z)$ and $\eta_1(z)$, viz. :

$$\eta_0(z) = A_0^{\pm}(z) M_0^{\pm}(z)$$
$$\eta_1(z) = A_0^{\pm}(z) M_1^{\pm}(z) \quad (20)$$

where

$$M_0^{\pm}(z) = \int d\sigma M^{\pm}(z,\sigma), \;\; M_1^{\pm}(z) = \int d\sigma \sigma M^{\pm}(z,\sigma). \quad (21)$$

Solving (20) and substituting the result into (18-19) yields finally $\eta(z,\sigma)$ via (17). Note that, since the bulk-phase densities $\eta_{\pm}(\sigma)$ must correspond to the same chemical potential (cf. (13)) :

$$\mu_0(\infty,\sigma;T,[\eta_+]) = \mu_0(-\infty,\sigma;T,[\eta_-]), \quad (22)$$

the equations (16-20) bearing the "+" sign are equivalent (but not identical) to those bearing the "-" sign. The above equations can therefore be used with either sign, the results will be the same provided, of course, that the two bulk phases are coexisting equilibrium phases.

To proceed we must specify $V_A(r;1,1)$. Since only fluid phases are involved the particular form of $V_A(r;1,1)$ is not very important and in view of (11) we will, for simplicity, take it to be gaussian or in the notation of [7] :

$$V_A(r;1,1) = -\epsilon(1,1)\, 8\, v(1)\, \frac{\exp(-b\,\overline{r}^2)}{R^3(1)\,(\frac{\pi}{b})^{3/2}} \;\; ; \;\; \overline{r} = \frac{r}{R(1)} \quad (23)$$

where $\epsilon(1,1)$ is a reference amplitude. If, $t = k_B T/\epsilon(1,1)$, denotes the dimensionless temperature eq. (11) yields on using (23) :

$$\beta V_1(|z|) = -\frac{8}{t}\, \frac{\exp(-b\,\overline{z}^2)}{R(1)\,(\frac{\pi}{b})^{1/2}}, \;\; \overline{z} = \frac{z}{R(1)} \;\; ; \;\; \beta V_0 = -\frac{8}{t}. \quad (24)$$

Below we have used (for convergence reasons) $b = 4$.

Finally, eq. (17) also requires explicit data for $\eta_{\pm}(\sigma)$. For the latter we will take the two-phase coexistence densities obtained in [7] for the same temperature (t) and for an initial parent-phase density, $\rho_0(\sigma) = \rho_0\, h_0(\sigma)$, of average density ρ_0 (or, in dimensionless form, $\eta_0 = \rho_0\, v(1)$) and a Schulz-Zimm size-distribution $h_0(\sigma)$:

$$h_0(\sigma) = \frac{\alpha^{\alpha}}{\Gamma(\alpha)} \sigma^{\alpha-1} exp(-\alpha\sigma) \quad (25)$$

where $\Gamma(\sigma)$ is the Euler gamma function and $I = 1 + (1/\alpha)$ the polydispersity index. Note that $1/\alpha = I - 1$ is the variance of $h_0(\sigma)$ so that $I = 1$ (or $\alpha = \infty$) corresponds to the monodisperse limit whereas the reference species $\sigma = 1$ corresponds to the average value of σ in the parent-phase. Of course, other size-distributions can be used but as shown in [6,7] the particular form of $h_0(\sigma)$ has little influence as long as it remains monomodal.

In the present work, we have studied two polydispersities, viz. $\alpha = 50$ ($I = 1.02$) and $\alpha = 15$ ($I = 1.07$), for several temperatures (t) and densities (η_0). In Fig. 1 we show three binodals of the bulk phase diagram for $\alpha = 50$ (see also [7]). In Fig. 2 we show the size-distributions of two bulk-phases coexisting for $t = 1$, $\eta_0 = 0.48$ and $\alpha = 15$. The inset of Fig. 2 shows the corresponding density distributions. It is seen there that for a range of σ-values ($0.3 \leq \sigma \leq 0.7$) the densities of the "low"-density phase actually exceed the corresponding densities of the "high"-density phase. Finally, in Fig. 3 we show a variety of density profiles for the non-uniform two-phase system. It is seen that, compared to the monodisperse case, the polydispersity widens the interfacial region. The results of Fig. 3 have been obtained by solving eq. (20) iteratively (e.g. by starting from a tanh-profile) whereas the results shown in Figs. 1-2 have been obtained as explained in [7].

IV. ADSORPTION PROPERTIES

In macroscopic thermodynamics it is customary to replace the continuous density profiles, $\eta(z,\sigma) = v(1)\,\rho(z,\sigma)$, obtained in Sec. III by discontinuous (with respect to z) profiles, $\overline{\eta}(z,\sigma) = v(1)\,\overline{\rho}(z,\sigma)$, of the form [4] :

$$\overline{\rho}(z,\sigma) = \rho_+(\sigma)\,\theta(z - z_G(\sigma)) + \rho_-(\sigma)\,\theta(z_G(\sigma) - z) + \Gamma(\sigma)\,\delta(z - z_G(\sigma)) \quad (26)$$

where $\eta_{\pm}(\sigma) = v(1)\,\rho_{\pm}(\sigma)$ are the density distributions of the two coexisting bulk phases and $\Gamma(\sigma)$ is the adsorption of species σ at the interface for which $z = z_G(\sigma)$ is the Gibbs dividing surface of species σ. In (26), $\theta(z)$ denotes the Heaviside step function and $\delta(z)$ the Dirac delta function. The macroscopic ($\overline{\rho}(z,\sigma)$) and microscopic ($\rho(z,\sigma)$) profiles can be adjusted by requiring them to satisfy :

$$\int_{-\infty}^{\infty} dz\, \{\rho(z,\sigma) - \overline{\rho}(z,\sigma)\} = 0 \quad (27)$$

which implies that $\Gamma(\sigma)$ be defined as the surface excess density, viz. :

$$\Gamma(\sigma) = \int_{-\infty}^{\infty} dz\, \{\rho(z,\sigma) - \hat{\rho}(z,\sigma)\} \quad (28)$$

where $\hat{\rho}(z,\sigma)$ is the following bulk-phase switch function :

$$\hat{\rho}(z,\sigma) = \rho_+(\sigma)\,\theta(z - z_G(\sigma)) + \rho_-(\sigma)\,\theta(z_G(\sigma) - z). \quad (29)$$

Since at $z = \pm\infty$ both densities match, $\rho(z = \pm\infty,\sigma) = \hat{\rho}(z = \pm\infty,\sigma) = \rho_{\pm}(\sigma)$, we can integrate (28) by parts and obtain :

$$\Gamma(\sigma) = \int_{-\infty}^{\infty} dz\,(z_G(\sigma) - z)\,\rho'(z,\sigma) \tag{30}$$

where $\rho'(z,\sigma) = \partial\rho(z,\sigma)/\partial z$. As seen from (30) the value of $\Gamma(\sigma)$ attributed to a given $\rho(z,\sigma)$ still depends on the value of $z_G(\sigma)$. Since there is no absolute determination possible for $z_G(\sigma)$ we have to fix it arbitrarily, e.g. for the reference species $\sigma = 1$. Taking henceforth $z_G(\sigma) \equiv z_G(1)$ for all σ we can fix $z_G(1)$ by requiring that the corresponding adsorption, $\Gamma(1)$, vanishes. Eq. (30) implies then :

$$z_G(1) = \frac{\int_{-\infty}^{\infty} dz\, z\,\rho'(z,1)}{\int_{-\infty}^{\infty} dz\,\rho'(z,1)} \tag{31}$$

whereas (30) becomes :

$$\Gamma_1(\sigma) = \int_{-\infty}^{\infty} dz\,(z_G(1) - z)\,\rho'(z,\sigma) \tag{32}$$

where the subscript 1 on $\Gamma(\sigma)$ indicates that the adsorption of species σ is referred to the zero-adsorption Gibbs dividing surface (31) of the reference species $\sigma = 1$, hence $\Gamma_1(1) = 0$. Since, moreover, the system is of infinite extend in the z-direction we may choose $z_G(1)$ as the origin of our coordinate system, i.e. $z_G(1) = 0$. Some examples of $\Gamma_1(\sigma)$ are given in Fig. 4. As seen from Fig. 4, at the interface there is both an excess of small particles ($\Gamma_1(\sigma) > 0$ for $\sigma < 1$) and a depletion of large particles ($\Gamma_1(\sigma) < 0$ for $\sigma > 1$) with an adsorption ($\Gamma_1(\sigma)$) which strongly depends on t and η_0.

V. PRESSURE PROFILE ACROSS THE PLANAR INTERFACE

Besides the density profile ($\rho(z,\sigma)$)which gives rise to the adsorption properties described in the previous section, an interface also involves a pressure profile ($p(z)$) which in turn gives rise to the surface tension as will be shown [9] in the next section. In order to expose the pressure in the interior of the interface described by $\rho(z,\sigma)$, we first cut this interface with a plane perpendicular to the density profiles, say the $x = 0$ plane, and remove the matter on the $x < 0$ side of this plane while leaving the matter on the $x \geq 0$ side intact. Such a semi-infinite system with a density, $\rho(\mathbf{r},\sigma) = \theta(x)\,\rho(z,\sigma)$, can be realized within the DFT of Sec.II by replacing the matter removed from the $x < 0$ half-space by a corresponding external field, say $\Phi(\mathbf{r},\sigma)$. The pressure acting normal to the $x = 0$ plane, i.e. acting in a direction which is tangential to the density profiles, can then be obtained by submitting the $x = 0$ plane to an infinitesimal non-uniform normal deformation, viz. $x \to x + \delta u(y,z)$, and computing the resulting thermodynamic work of deformation (cf. [9]). Since during this infinitesimal deformation, $\Phi(\mathbf{r},\sigma) \to \Phi(\mathbf{r},\sigma) + \delta\Phi(\mathbf{r},\sigma)$ and $\rho(\mathbf{r},\sigma) \to \rho(\mathbf{r},\sigma) + \delta\rho(\mathbf{r},\sigma)$, the system has to remain in equilibrium at the given T and $\mu(\sigma)$, the relation between $\delta\Phi(\mathbf{r},\sigma)$ and $\delta\rho(\mathbf{r},\sigma)$ can be obtained from the equilibrium condition (3) as :

$$\delta\mu(\sigma) = 0 = \delta\Phi(\mathbf{r},\sigma) + \int d\mathbf{r}' \int d\sigma' \frac{\delta^2 F(T,[\rho])}{\delta\rho(\mathbf{r},\sigma)\,\delta\rho(\mathbf{r}',\sigma')}\,\delta\rho(\mathbf{r}',\sigma'). \tag{33}$$

The resulting thermodynamic work of deformation, δA, can then be obtained from (1) :

$$\delta A|_{T,[\mu]} = \int d\mathbf{r} \int d\sigma\,\rho(\mathbf{r},\sigma)\,\delta\Phi(\mathbf{r},\sigma) \tag{34}$$

or on using (33), from :

$$\delta A|_{T,[\mu]} = -\int d\mathbf{r} \int d\sigma \int d\mathbf{r}' \int d\sigma'\,\rho(\mathbf{r},\sigma) \frac{\delta^2 F(T,[\rho])}{\delta\rho(\mathbf{r},\sigma)\,\delta\rho(\mathbf{r}',\sigma')}\,\delta\rho(\mathbf{r}',\sigma'). \tag{35}$$

Since in the present geometry we have, $\delta\rho(\mathbf{r},\sigma) = \rho(x + \delta u(y,z), y, z, \sigma) - \rho(x,y,z,\sigma) = \delta u(y,z)\,.(\partial\rho(\mathbf{r},\sigma)/\partial x) + O(\delta u^2)$, eq. (35) can be rewritten after dropping the $O(\delta u^2)$ term:

$$\delta A|_{T,[\mu]} = -\int dy' \int dz'\,\delta u(y',z')\,p(y',z') \tag{36}$$

which defines the pressure $p(y,z)$ acting at $\mathbf{r} = (0,y,z)$ in a direction normal to the $x = 0$ plane. Indeed, since $\delta u(y,z)$ is arbitrary (35-36) imply :

$$p(y,z) = \int dx \int d\sigma \int d\mathbf{r}' \int d\sigma'\,\rho(\mathbf{r}',\sigma') \frac{\delta^2 F(T,[\rho])}{\delta\rho(\mathbf{r}',\sigma')\,\delta\rho(\mathbf{r},\sigma)}.\frac{\partial\rho(\mathbf{r},\sigma)}{\partial x} \tag{37}$$

where, for convenience, we have interchanged the role of the primed and unprimed variables. In the present vdW-approximation we obtain from (4) :

$$\frac{\delta^2 F(T,[\rho])}{\delta\rho(\mathbf{r},\sigma)\,\delta\rho(\mathbf{r}',\sigma')} = k_B\,T\frac{\delta(\mathbf{r}-\mathbf{r}')\,\delta(\sigma-\sigma')}{\rho(\mathbf{r},\sigma)} + V_A(|\mathbf{r}-\mathbf{r}'|;\sigma,\sigma') + k_B\,T\,\frac{\delta(\mathbf{r}-\mathbf{r}')}{E(\mathbf{r},[\rho])}\{v(\sigma) + v(\sigma') + \frac{v(\sigma)\,v(\sigma')}{E(\mathbf{r},[\rho])}\int d\sigma''\,\rho(\mathbf{r},\sigma'')\} \tag{38}$$

which on behalf of (7), reduces here to :

$$\frac{\delta^2 F(T,[\rho])}{\delta\rho(\mathbf{r},\sigma)\,\delta\rho(\mathbf{r}',\sigma')} = k_B\,T\frac{\delta(\mathbf{r}-\mathbf{r}')\,\delta(\sigma-\sigma')}{\rho(\mathbf{r},\sigma)} + \sigma\sigma'\,V_A(|\mathbf{r}-\mathbf{r}'|;1,1) + k_B\,T\,\delta(\mathbf{r}-\mathbf{r}')\,v(1)\{\frac{1+E(\mathbf{r},[\rho])}{(E(\mathbf{r},[\rho]))^2}\} \tag{39}$$

so that (37) can be rewritten :

$$p(y,z) = \int dx \int d\sigma \{ k_B\, T \frac{\partial \rho(\mathbf{r},\sigma)}{\partial x} + \int d\mathbf{r}' \int d\sigma'\, \rho(\mathbf{r}',\sigma')\, V_A(|\mathbf{r}-\mathbf{r}'|;\sigma,\sigma') \frac{\partial \rho(\mathbf{r},\sigma)}{\partial x} + k_B\, T\, v(1)\, \rho(\mathbf{r},\sigma) \frac{(1+E(\mathbf{r},[\rho]))}{(E(\mathbf{r},[\rho]))^2} \int d\sigma' \frac{\partial \rho(\mathbf{r},\sigma')}{\partial x} \}. \quad (40)$$

Taking into account that here, $\rho(\mathbf{r},\sigma) = \theta(x)\,\rho(z,\sigma)$, we can rewrite (40) as :

$$v(1)\, p(y,z) = k_B\, T \int_{-\infty}^{\infty} dx \frac{\partial}{\partial x} \{ \frac{\eta_0(z)\,\theta(x)}{1-\eta_0(z)\,\theta(x)} \} + \int_{-\infty}^{\infty} dx \int d\mathbf{r}'\, V_A(|\mathbf{r}-\mathbf{r}'|;1,1)\, \delta(x)\, \eta_1(z)\, \theta(x')\, \eta_1(z') \quad (41)$$

where $\eta_0(z)$ and $\eta_1(z)$ have been defined in (10). Eq. (41) can be rewritten as :

$$v(1)\, p(z) = \frac{k_B T\, \eta_0(z)}{1-\eta_0(z)} + \frac{1}{2}\, \eta_1(z) \int_{-\infty}^{\infty} dz' V_1(|z-z'|)\, \eta_1(z') \quad (42)$$

where $V_1(|z|)$ was defined in (11) and we took into account that $p(y,z)$ is independant of y as expected from the translational invariance in the y-direction. We finally rewrite (42) in a manner similar to (8) :

$$v(1)\, p(z) = v(1)\, p_0(z;T,[\eta]) + \frac{1}{2}\, \eta_1(z) \int_{-\infty}^{\infty} dz' V_1(|z-z'|)\, \{\eta_1(z') - \eta_1(z)\} \quad (43)$$

with, $p_0(z;T,[\eta])$, a shorthand notation for :

$$v(1)\, p_0(z;T,[\eta]) = \frac{k_B T\, \eta_0(z)}{1-\eta_0(z)} + \frac{1}{2}\, V_0\, (\eta_1(z))^2 \quad (44)$$

where V_0 was defined in (11). It is seen that (44) represents the usual vdW-pressure of a uniform (polydisperse) system evaluated for the local density $\eta(z,\sigma)$, while the same is true of (9) for the chemical potential. From (40) it is seen that the local pressure $p(z)$ is completely determined by the local density $\eta(z,\sigma)$. From (43) and $\eta(\pm\infty,\sigma) = \eta_\pm(\sigma)$ we obtain $p(\pm\infty) = p_0(\pm\infty;T,[\eta_\pm])$, but since $\eta_\pm(\sigma)$ must satisfy [7] :

$$\frac{k_B T\, \eta_0^+}{1-\eta_0^+} + \frac{1}{2}\, V_0\, (\eta_1^+)^2 = \frac{k_B T\, \eta_0^-}{1-\eta_0^-} + \frac{1}{2}\, V_0\, (\eta_1^-)^2 \quad (45)$$

together with (22), we have $p(\infty) = p(-\infty)$, or $\int dz\, p'(z) = 0$, which expresses the stability of the planar interface (cf. [9] for details).

Some of the pressure profiles, $p(z)$, obtained from (43) using the density profiles of Sec. III are shown in Fig. 5. While $p(z)$ remains constant in the bulk phases it exhibits a structure in the interfacial region which is more pronounced for the lower temperatures and disappears gradually when $t = t_c$ is approached. This structure consists of a pressure depletion on the high-density side of the interface and a pressure excess on the low-density side (a similar structure was found in the monodisperse case [8] for a different potential $V_A(r;1,1)$ and was seen also in the simulation results of [13]). This local structure of $p(z)$ reflects a competition between the characteristic length-scales of $\rho(z,\sigma)$ and of $V_A(r;1,1)$. It is also seen (compare Figs. 5(a) and (b)) that increasing the polydispersity (i.e. lowering α) widens the interfacial region (i.e. the region where $p'(z) \neq 0$).

VI. SURFACE TENSION AND SURFACE OF TENSION

In a way analoguous to (26), the microscopic pressure profile $p(z)$ of Sec. V is replaced in macroscopic thermodynamics by a discontinuous pressure profile, $\overline{p}(z)$:

$$\overline{p}(z) = p_+\, \theta(z-z_0) + p_-\, \theta(z_0-z) - \gamma\, \delta(z-z_0) \quad (46)$$

where $p_\pm = p(\pm\infty)$ denote the bulk-phase pressures and γ is the surface tension acting on a surface of tension located at $z = z_0$. As in (27) the two profiles can be adjusted by requiring that:

$$\int_{-\infty}^{\infty} dz\, \{p(z) - \overline{p}(z)\} = 0 \quad (47)$$

which on behalf of (46) yields :

$$\gamma = \int_{-\infty}^{\infty} dz\, \{\hat{p}(z) - p(z)\} \quad (48)$$

where $\hat{p}(z)$:

$$\hat{p}(z) = p_+\, \theta(z-z_0) + p_-\, \theta(z_0-z) \quad (49)$$

is the switch function for the bulk-phase pressure (cf. (29)). Integrating (48) by parts and taking into account that for a planar interface we must have, $p(\pm\infty) = \hat{p}(\pm\infty) = p_\pm$ together with $p_+ = p_-$, yields:

$$\gamma = \int_{-\infty}^{\infty} dz\, z\, p'(z) \quad (50)$$

which shows that γ can be determined from the knowledge of $p'(z) = dp(z)/dz$ alone, i.e. without knowing z_0 (cf. the difference with (30)), a feature specific to the planar interface (cf. [9]). To determine z_0 one can nevertheless also impose (cf. [9]) that :

$$\int_{-\infty}^{\infty} dz\, z\, \{p(z) - \overline{p}(z)\} = 0 \quad (51)$$

which on using (47) can be rewritten as :

$$0 = \int_{-\infty}^{\infty} dz\,(z-z_0)\,\{p(z)-\overline{p}(z)\}$$
$$= \int_{-\infty}^{\infty} dz\,(z-z_0)\,\{p(z)-\hat{p}(z)\} \qquad (52)$$

or integrating (52) by parts and using $p_+ = p_-$ one obtains :

$$\int_{-\infty}^{\infty} dz\,(z-z_0)^2\,p'(z) = 0. \qquad (53)$$

Using, $\int dz\,p'(z) = 0$, eq. (53) yields finally :

$$z_0 = \frac{1}{2}\,\frac{\int_{-\infty}^{\infty} dz\,z^2\,p'(z)}{\int_{-\infty}^{\infty} dz\,z\,p'(z)} \qquad (54)$$

so that both γ and z_0 can be obtained from $p'(z)$ (cf. (50) and (54)).

Fig. 6 shows some of the results obtained for γ using the pressure profiles of Sec. V. From Fig. 6a it is seen that γ decreases when increasing η_0 at a fixed polydispersity. When, instead, the polydispersity is changed starting from the monodisperse case ($\alpha = \infty$) there are two competing effects (cf. Fig. 6b) : the polydispersity tends to lower the surface tension but at the same time it raises the critical-point temperature since the polydispersity favors the phase separation (cf. [7]). As a net result of this competition the surface tension of the polydisperse system is lower than that of the monodisperse one for $t < t_0$ but exceeds it for $t > t_0$ with a crossover temperature t_0 which increases with the polydispersity. To show this more clearly Fig. 6c displays γ versus $t/t_c(\alpha)$, where $t_c(\alpha)$ is the critical point temperature of the system with polydispersity α.

The above surface tension (γ) acts on the surface of tension located at $z = z_0$ (cf. eq. (46)). From Fig. 7 it is seen that $z_0 < 0$, i.e. the surface of tension is different from the zero-adsorption Gibbs dividing surface ($z = z_G(1) = 0$) and located on the high-density side of this interface (this can also be seen from Fig. 5). The fact that $z_0 \neq z_G(1)$ points to a fundamental inadequacy of the macroscopic description of interfaces (cf. [9]) since two different quantities are used to locate the interface on a macroscopic level. The quantity, $l_T = z_G(1) - z_0$, is usually called Tolman's length [4]. Finally, from Fig. 8 it is seen that on approaching the critical point γ vanishes with a classical critical exponent ($= 3/2$) as expected from the mean-field vdW-theory [4].

VII. CONCLUSIONS

We have studied the planar interface resulting from the phase separation or fractionation of a parent phase of a polydisperse colloidal system into a low-density fluid phase enriched in small particles and a high-density fluid phase enriched in large particles. In order to tackle the combined effect of the system's polydispersity and spatial non-uniformity we have kept the theorical description as simple as possible but are confident that similar results can be found from more involved descriptions. Using a simple van der Waals description [7-8] to model the polydisperse non-uniform system of spherical colloidal particles with excluded volume repulsions and gaussian attractions it was found that the small particles accumulate at the interface, the latter being moreover depleted with larger particles and broadened with respect to the monodisperse case. We also found that for a given temperature the surface tension is the result of a competition between two polydispersity-induced effects, namely its tendancy to lower the surface tension and at the same time to raise the critical point temperature, with the former effect winning at low-temperatures and the latter at higher temperatures. Finally, the surface of tension was found to be located on the high-density side of the interface pointing to a positive Tolman's length.

Acknowledgements
M.B. acknowledges financial support from the F.N.R.S.

[1] S. Chandrasekhar, *Liquids Crystals*, (Cambridge University Press, Cambridge, 1992); H.G. Elias, *An introduction to Polymer Science*, (VCH Publishers, Inc., Weinhein, 1997); W.B. Russel, D.A. Saville and W.R. Schowalter, *Colloidal Dispersions*, (Cambridge University Press, Cambridge, 1998).

[2] J.L. Barrat and J.P. Hansen, *J. Physique* **47**, 1547(1986); R. McRae and A.D.J. Haymet, *J. Chem. Phys.* **88**, 1114(1988); P. Bartlett, *J. Chem. Phys.* **107**, 188(1997); S.E. Phan, W.B. Russel, J. Zhu and P.M. Chaikin, *J. Chem. Phys.*, **108**, 9789(1998); R.M.L. Evans, D.J. Fairhurst and W.C.K. Poon, *Phys. Rev. Lett.* **81**,1326(1998); P.B. Warren, *Phys. Rev. Lett.* **80**, 1369(1998); R.P. Sear, *Europhys. Lett.* **44**, 531(1998); P. Sollich and M.E. Cates, *Phys. Rev. Lett.* **80**, 1365(1998); S. Leroch, G. Kahl and F. Lado, *Phys. Rev. E* **59**, 6937(1999); P. Bartlett and P.B. Warren, *Phys. Rev. Lett.* **82**,1979(1999); P.B. Warren, *Europhys. Lett.* **46**, 295(1999); J.A. Cuesta, *Europhys. Lett.* **46**, 197(1999); R.M.L. Evans, *Phys. Rev. E* **59** , 3192(1999); H. Xu and M. Baus, *Phys. Rev. E* **61** , 3249(2000); P.A. Monson and D.A. Kofke, *Adv. Chem. Phys.* **115**, 113(2000); P. Sollich, P.B. Warren and M. E. Cates, *Adv. Chem. Phys.* **116**, 265 (2001); D. Goulding and J.P. Hansen, *Molec. Phys.* **99**, 865(2001).

[3] I. Pagonabarraga, M.E. Cates and G.J. Ackland, *Phys. Rev. Lett.* **84**, 911(2000).

[4] J.S. Rowlinson and B. Widom, *Molecular Theory of Capillarity*, (Clarendon, Oxford, 1982).

[5] R.J. Hunter, *Foundations of colloid science*, (Clarendon

Press, Oxford, 1993).
[6] L. Bellier-Castella, M. Baus and H. Xu, *J. Chem. Phys.* **115**, 3381(2001).
[7] L. Bellier-Castella, H. Xu and M. Baus, *J. Chem. Phys.* **113**, 8337(2000).
[8] R. Lovett and M. Baus, *J. Chem. Phys.* **111**, 5544(1999); M. Baus and R. Lovett, ibid **111**, 5555(1999).
[9] R. Lovett and M. Baus, *Adv. Chem. Phys.* **102**, 1(1997) and references therein.
[10] J. P. Hansen and I.R. Mc Donald, *Theory of simple liquids*, (2^d edition), (Academic Press, London, 1986).
[11] J.A. Gualtieri, J.M. Kincaid and G. Morrison, *J. Chem. Phys.* **77**, 521(1982); J.J. Salacuse and G. Stell. *J. Chem. Phys.* **77**, 3714(1982); J.B. Briano and E.D. Glandt, *J. Chem. Phys.* **80**, 3336(1984); R. Aris and G.R. Gavalas, *Philos. Trans. R. Soc. London Ser.A* **260**, 351(1966).
[12] A. Daanoun, C.F. Tejero and M. Baus, *Phys. Rev. E* **50**, 2913(1994); T. Coussaert and M. Baus, *Phys. Rev. E* **52**, 862(1995); A. Oukouiss and M. Baus, *Phys. Rev. E* **55**, 7242(1997); R. Achrayah and M. Baus, *Phys. Rev. E* **57**, 4361(1998); R. Lovett and M. Baus, *J. Chem. Phys.* **111**, 5544(1999).
[13] M. Mareschal, M. Baus and R. Lovett, *J. Chem. Phys.* **106**, 645(1997); H. El Bardouni, M. Mareschal, R. Lovett and M. Baus, ibid **113**, 9804(2000).

Figure Captions

FIG. 1. The temperature (t)-density (η) bulk-phase diagram for $\alpha = 50$ (cf. [7]). Three binodals are shown. They correspond to the parent-phase densities $\eta_0 = 0.3$ (dashed line), $\eta_0 = \eta_c = 0.3659$ (full line) and $\eta_0 = 0.45$ (dot-dashed line). Two binodals are truncated upwards at resp. the supra-critical temperature $t \simeq 1.246$ (for $\eta_0 = 0.3$) and the infra-critical temperature $t \simeq 1.1905$ (for $\eta_0 = 0.45$) while the untruncated binodal passes through the critical point $t_c = 1.2355$, $\eta_c = 0.3659$. Similar results are obtained (cf. [7]) for $\alpha = 15$ in which case the critical point corresponds to $t_c = 1.2889$, $\eta_c = 0.4842$.

FIG. 2. The density-($\eta_\pm(\sigma) = \eta_\pm\, h_\pm(\sigma)$; cf. inset) and size-distributions ($h_\pm(\sigma)$) of the low-density (η_+; full line) and the high-density (η_-; dashed line) bulk phases ($\eta_+ < \eta_-$) which coexist for $t = 1$, $\eta_0 = \eta_c = 0.4842$ and $\alpha = 15$. Note from the inset that for, $0.3 \lesssim \sigma \lesssim 0.7$, the behaviors of $\eta_\pm(\sigma)$ and $\eta_\pm = \int d\sigma\, \eta_\pm(\sigma)$ are reversed, i.e. although $\eta_+ < \eta_-$ we have $\eta_+(\sigma) > \eta_-(\sigma)$ for these σ-values. The low (high)-density phase is enriched in small (large) particles.

FIG. 3. Density profiles for $\alpha = 15$ across a planar interface : (a)-(b) at constant temperature ($t = 1$) and (c) at constant density ($\eta_0 = \eta_c = 0.4842$). In (a) we show $\eta_0(z)$ (full line) and $\eta_1(z)$ (dotted line). Also shown for comparison is the monodisperse case (dashed line) corresponding to $\alpha = \infty$ and $\eta_0(z) \equiv \eta_1(z)$. It is seen that the polydispersity broadens the interface. In (b) we show $\eta(z, \sigma)$ for $\sigma = 1.25$ (dot-dashed), $\sigma = 1$ (dashed), $\sigma = 0.75$ (dotted) and $\sigma = 0.65$ (full line). It is seen that the small particles ($\sigma < 1$) accumulate in the interfacial region. Note also that $\eta_+(0.65) > \eta_-(0.65)$ whereas $\eta_+(0.75) < \eta_-(0.75)$ in agreement with the reversal seen in Fig. 2. In (c) we show $\eta(z, \sigma = 0.65)$ for $\alpha = 15$, $\eta_0 = 0.4842$ and $t = 0.85$ (full line), 1 (dots), 1.1 (short dashes), 1.2 (long dashes) and 1.28 (dot-dash). (Here $z^* = (z - z_G(1))/R(1)$).

FIG. 4. The adsorption $\Gamma_1(\sigma)$ of σ-particles relative to the zero-adsorption Gibbs dividing surface ($z_G(1)$) of the reference particle ($\sigma = 1$) at (a) fixed density and (b) fixed temperature. Panel (a) corresponds to $\alpha = 15$, $\eta_0 = 0.4842$ and $t = 0.90$ (full line) 1.00 (dots), 1.10 (short dashes), 1.20 (long dashes), 1.28 (dot-dash). Panel (b) corresponds to $\alpha = 50$, $t = 1.15$ and $\eta_0 = 0.45$ (line), 0.3659 (dots), 0.3 (dashes). Note the rapid variations with t and η_0 of the interfacial excess of the small particles ($\sigma < 1$) and depletion of the large particles ($\sigma > 1$). (Here $\Gamma_1^*(\sigma) = \Gamma_1(\sigma).\, v(1)/R(1)$.)

FIG. 5. The pressure profile ($p(z)$) versus the distance (z) from a planar interface perpendicular to z-axis for (a) $\alpha = 50$ and $\eta_0 = 0.3659$ and (b) $\alpha = 15$ and $\eta_0 = 0.4842$ and three temperatures $t = 0.9$ (full line), $t = 1$ (dots) and $t = 1.1$ (dot-dashes). The interfacial region is seen to be broadened by the polydispersity. All profiles exhibit a pressure depletion (excess) on the high (low) density side of the interface. (Here $p^*(z) = p(z)\, v(1)/\epsilon(1,1)$ and $z^* = z/R(1)$.)

FIG. 6. The surface tension (γ) versus the temperature (t) for : (a) $\alpha = 50$ and $\eta_0 = 0.3$ (dots), $\eta_0 = \eta_c = 0.3659$ (full line) and $\eta_0 = 0.45$ (dot-dash); (b) $\alpha = 15$ (dot-dash), $\alpha = 50$ (dots) and $\alpha = \infty$ (full line) for $\eta_0 = \eta_c(\alpha)$; (c) the same as (b) but plotted now versus $t/t_c(\alpha)$ where $t_c(\alpha)$ and $\eta_c(\alpha)$ are, respectively, the (reduced) critical-point temperature and density of a system with polydispersity index $I = 1 + (1/\alpha)$. (Here $\gamma^* = \gamma\, v(1)/\epsilon(1,1))\, R(1)$.)

FIG. 7. Tolman's length ($l_T = z_G(1) - z_0$) versus the temperature (t) for $\alpha = 50$ and $\eta_0 = 0.3$ (dots), $\eta_0 = \eta_c = 0.3659$ (dash) and $\eta_0 = 0.45$ (dot-dash). (Here $l_T^* = l_T/R(1)$.)

FIG. 8. A $ln\,\gamma^*$ versus $ln\,t^*$ plot for $\alpha = \infty$ (full line) and $\alpha = 15$, $\eta_0 = \eta_c = 0.4842$ (dot-dash). In both cases the critical exponent (=3/2) of γ is classical. (Here $t^* = (t_c(\alpha) - t)/t_c(\alpha)$.)

Fig. 1 , Bellier-Castella et al., PRE

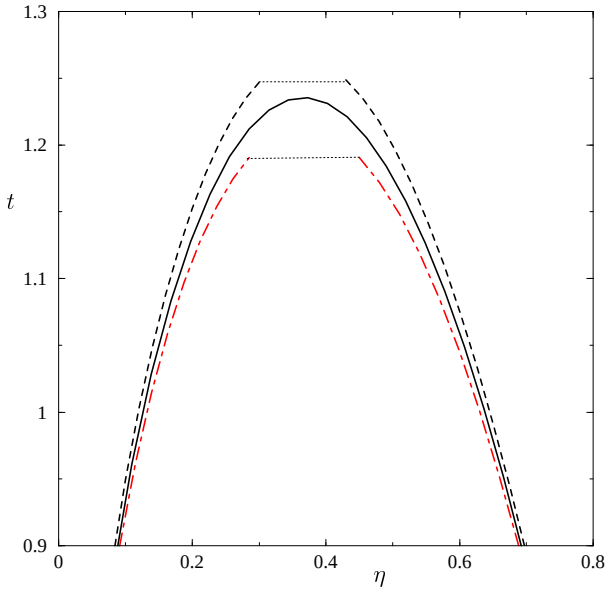

Fig. 2 , Bellier-Castella et al., PRE

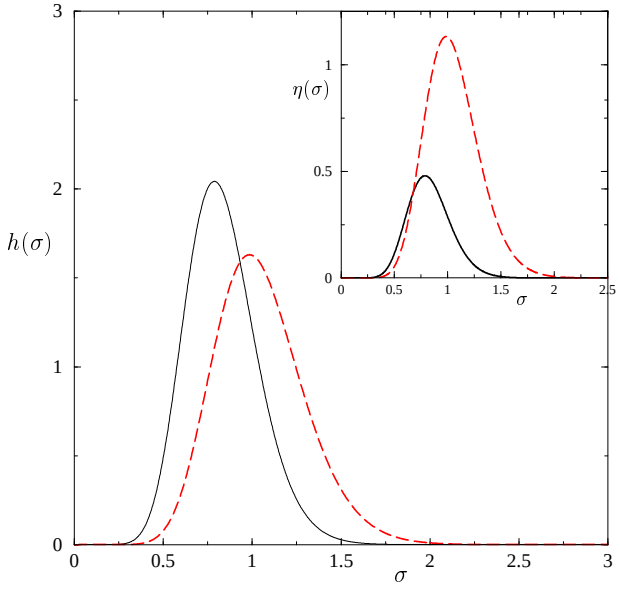

Fig. 3 , Bellier-Castella et al., PRE

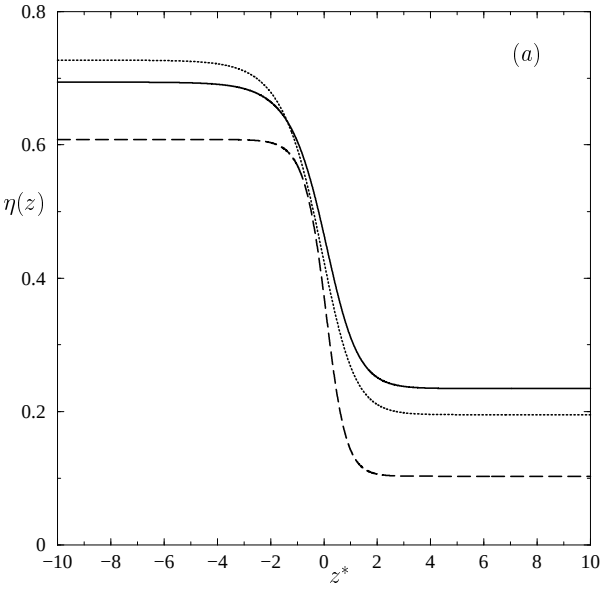

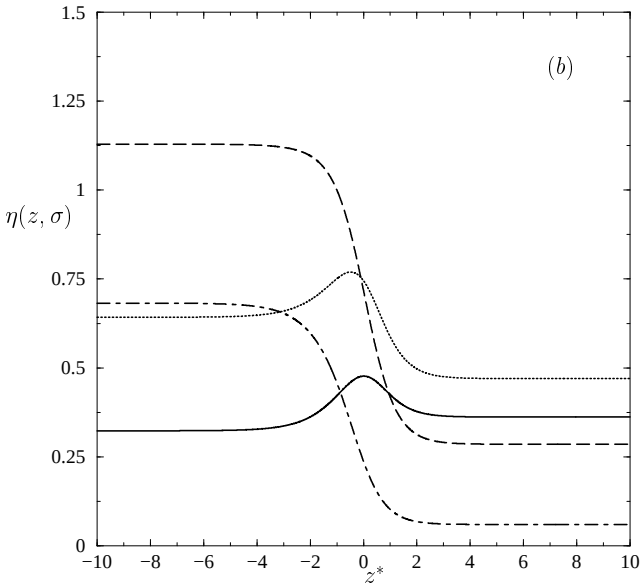

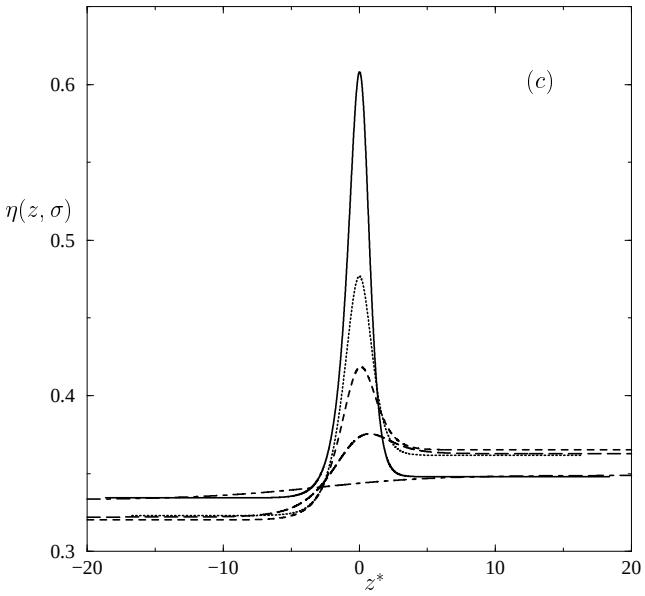
(c)
0.6
0.5
0.4
0.3
$\eta(z,\sigma)$
−20
−10
0
10
20
z^*

Fig. 4 , Bellier-Castella et al., PRE

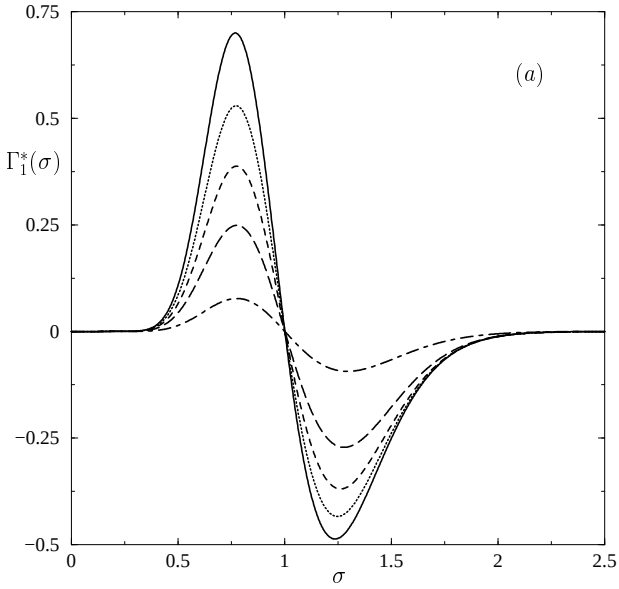

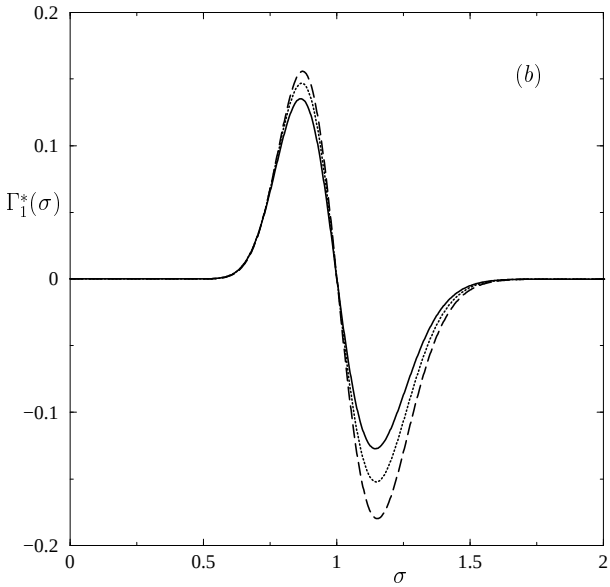

Fig. 5 , Bellier-Castella et al., PRE

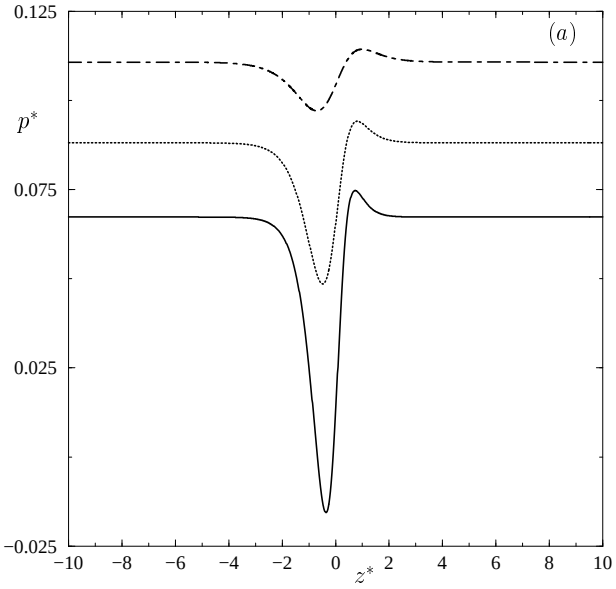

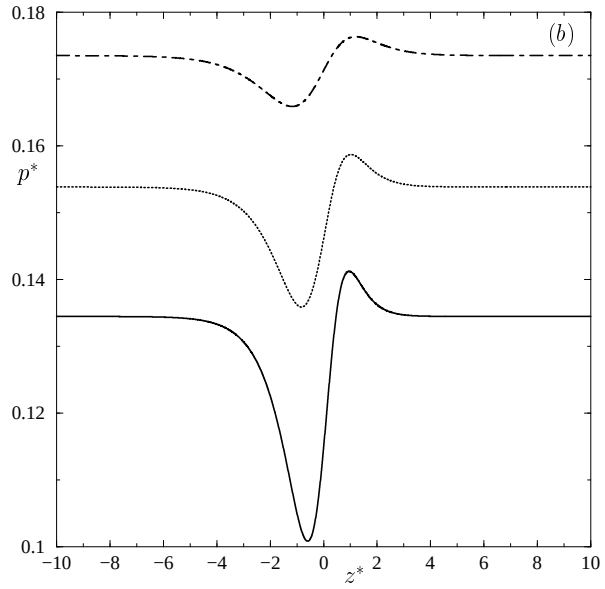

Fig. 6 , Bellier-Castella et al., PRE

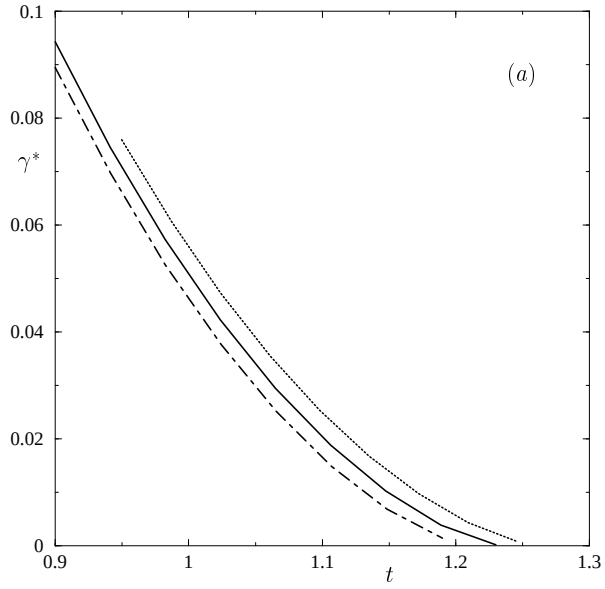

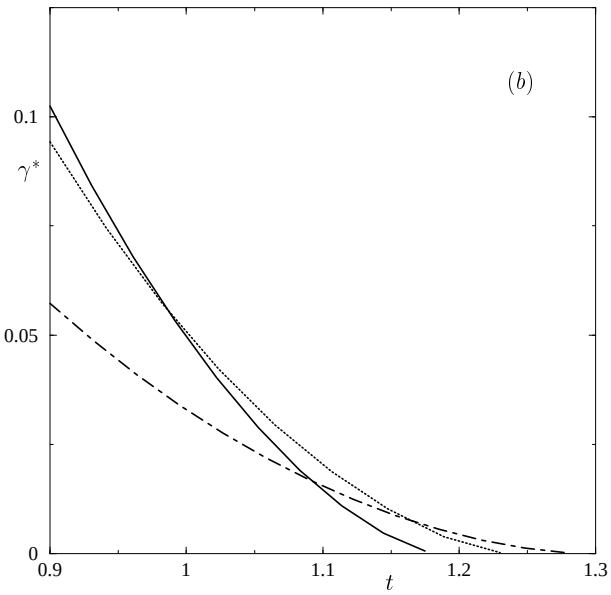

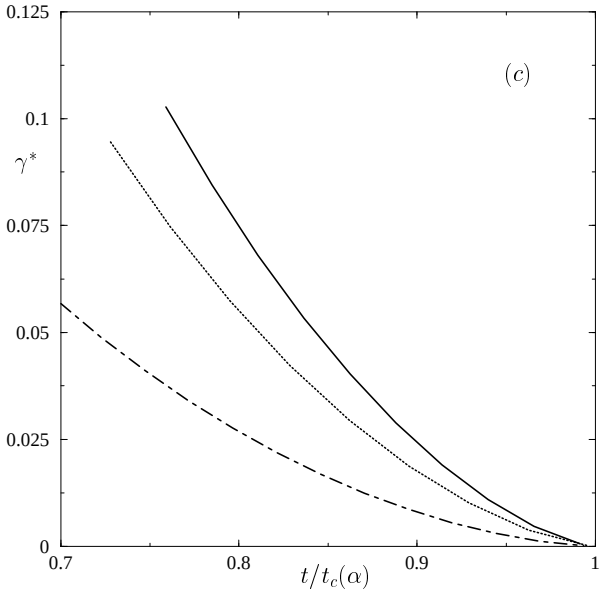
0.125
0.1
0.075
0.05
0.025
0
γ^*
0.7
0.8
0.9
1
$t/t_c(\alpha)$
(c)

Fig. 7 , Bellier-Castella et al., PRE

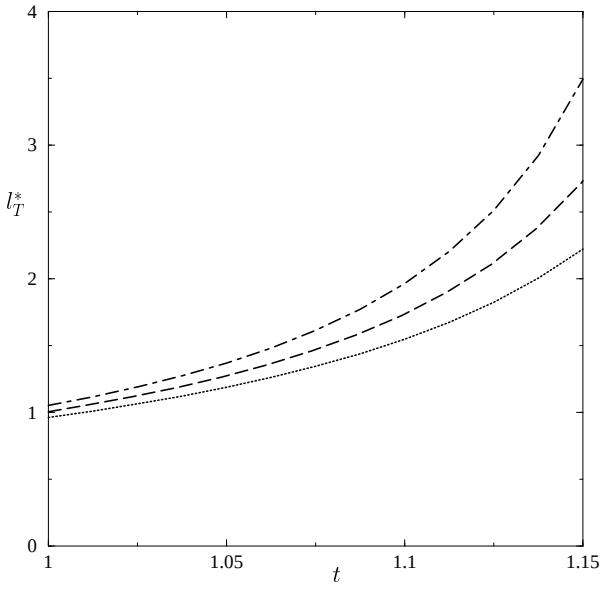

Fig. 8 , Bellier-Castella et al., PRE